



Combustion characteristics of a single decane/ethanol emulsion droplet and a droplet group under puffing conditions

J. Shinjo^{a,b,*}, J. Xia^a

^a *Department of Mechanical, Aerospace and Civil Engineering, and Institute of Energy Futures, Brunel University London, Uxbridge UB8 3PH, United Kingdom*

^b *Department of Mechanical, Electrical and Electronic Engineering, Shimane University, 1060 Nishikawatsu, Matsue 690-8504, Japan*

Received 28 November 2015; accepted 30 June 2016

Available online 16 July 2016

Abstract

Combustion characteristics of an ethanol-in-decane emulsion droplet and a droplet group under puffing conditions have been investigated by direct numerical simulation (DNS). Before puffing, a quasi-steady flame is formed in the wake of the parent decane droplet. Due to superheating, boiling of ethanol sub-droplets is initiated. Following rapid growth of the vapor bubble, ethanol vapor is unsteadily ejected out and interacts with the downstream wake flame. The local gas mixture fraction is affected by this ejection. The gas-phase temperature and reaction rate also show different characteristics from those of a 1D steady flame. In the dual-fuel system, fuel/air mixing in combustion can be characterized by the scalar dissipation rates (SDRs) due to mixing of decane/air and ethanol/air and cross mixing of decane/ethanol. The transient interaction between the droplet wake flame and the ejected vapor by puffing is evident in the flame S-curves. The interaction is further quantified by the budget analysis in the mixture fraction – SDR space. The contribution of the cross SDR between decane and ethanol to the rate of change of the SDR of the primary fuel decane is initially negative, which is particular to puffing. Later the cross SDR can also become positive. As the mixing continues, the magnitude of the SDRs becomes smaller. When puffing occurs in the transverse direction, the ejected vapor may sweep a region within a few diameters away from the parent decane droplet. If other emulsion droplets are in this region of influence, inter-droplet interactions occur. A multiple-droplet case demonstrates this interaction and implies that such an interaction will occur in an emulsion fuel spray and should be considered in modeling a multi-component emulsion fuel spray in a combustor.

© 2016 The Author(s). Published by Elsevier Inc. on behalf of The Combustion Institute.

This is an open access article under the CC BY license. (<http://creativecommons.org/licenses/by/4.0/>)

Keywords: Emulsion droplets; Droplet combustion; Puffing; Vapor/flame interaction; Droplet grouping

* Corresponding author at: Department of Mechanical, Electrical and Electronic Engineering, Shimane University 1060 Nishikawatsu, Matsue 690-8504, Japan.

<http://dx.doi.org/10.1016/j.proci.2016.06.191>

1540-7489 © 2016 The Author(s). Published by Elsevier Inc. on behalf of The Combustion Institute. This is an open access article under the CC BY license. (<http://creativecommons.org/licenses/by/4.0/>)

E-mail address: jshinjo@ecs.shimane-u.ac.jp
(J. Shinjo).

1. Introduction

Reducing emissions of carbon dioxide (CO₂) and soot from liquid fuel combustion is significantly important due to increasing environmental concerns. Using biofuels such as bioethanol or biodiesel is one of the effective ways for reducing harmful emissions. Adding bioethanol to diesel is one possible solution for diesel engines [1,2]. Ethanol is oxygenated, i.e. an ethanol molecule contains an oxygen atom, which contributes to reducing particulate matter (PM). The miscibility of ethanol in diesel can be improved by adding biodiesel into the blend, which works as a surfactant agent. The blend forms ethanol-in-diesel emulsion, with ethanol dispersed as tiny sub-droplets in the continuous phase of diesel. Above a certain threshold of the ethanol-to-diesel ratio, puffing or microexplosion occurs due to the distinctly different boiling temperature of the two fuels. Following explosive boiling of superheated ethanol sub-droplets, puffing (partial microexplosion) causes partial droplet breakup and microexplosion violent breakup of the entire droplet [3–5]. When puffing or microexplosion occurs in a fuel spray, secondary atomization will be induced. Generally, secondary atomization enhances droplet evaporation and fuel/air mixing. Although with a great potential, our understanding on secondary atomization induced by puffing and microexplosion is still far from sufficient. It is therefore significantly important to understand the combustion characteristics of such fuel blends under puffing conditions for better and further utilization of biofuels. This is a complex physical problem on fluid and combustion dynamics, which is highly worth tackling.

In our previous DNS studies [5–7], physical mechanisms related to emulsion droplet puffing/microexplosion have been unveiled comprehensively, including vapor bubble growth and droplet breakup [5], convective heating of an emulsion droplet [6], and convective fuel-vapor/air mixing for a single emulsion droplet and a droplet group [7]. From these results, fuel-vapor/air mixing characteristics under puffing conditions have been unveiled for non-reacting emulsion fuel droplets. The objective of the present study is to investigate combustion dynamics of emulsion droplets, especially focusing on (1) interactions between puffing ethanol vapor and droplet combustion using scalar dissipation rates (SDRs) as a primary physical and modeling parameter and (2) change of droplet group combustion characteristics due to puffing. To simplify the combustion kinetics and the boiling temperature property, decane is used as a surrogate fuel, and decane/ethanol emulsion is considered. Our in-house experimental study has confirmed that the droplet combustion characteristics are similar using decane. Using an enlarged-scale

single emulsion droplet (diameter $D \sim 2$ mm) [7], it has been shown that the local flame luminosity increases transiently when puffing occurs, due to the modulated local equivalence ratio by the ejected ethanol vapor. Such a flame/vapor interaction is also expected to occur in a fuel spray. To directly relate the present results to droplets in a fuel spray, typical spray-scale droplets of $D \sim O(10 \mu\text{m})$ are considered, as in [5–7]. Both a single decane/ethanol emulsion droplet and a droplet group are considered. As pointed out in [8], the time of heating for spray-scale droplets in a combustor is generally short, and puffing is more likely to occur than complete microexplosion. Therefore puffing effects on combustion characteristics of an emulsion fuel droplet and a droplet group are investigated.

2. Mathematical formulations, numerical methods, and case setup

The governing equations are the conservation equations of mass, momentum, energy and species mass fractions [5–7]. The energy equation is transformed into the temperature equation. Compressibility is included to account for explosive boiling and thermal expansion. Newton's viscosity law is used and heat conduction is modeled by Fourier's law. Mass diffusion is modeled by Fick's law with a unity Lewis number in the gas phase. Temperature-dependent physical properties to cover the necessary temperature range are retrieved from the database of NIST (National Institute of Standards and Technology) [9].

The rate of phase change $\dot{\omega}_p$ is formulated at an evaporating or boiling interface, which is resolved in the grid system, as [5–7,10]

$$h_l \dot{\omega}_p = [\lambda \nabla T \cdot \mathbf{n}], \quad (1)$$

$$\dot{\omega}_p (Y_{i,G} - Y_{i,L}) = [\rho D_{diff} \nabla Y_i \cdot \mathbf{n}], \quad (2)$$

where h_l is the latent heat of evaporation, λ the thermal conductivity, D_{diff} the diffusion coefficient and \mathbf{n} the surface-normal unit vector. The subscript L denotes the liquid phase and G the gas phase, respectively. The square brackets denote the difference of a variable f between the liquid and gas phases at the interface, i.e. $[f] = f_L - f_G$. For the evaporation on the surface of the parent decane droplet, the Clapeyron–Clausius relation is used [5–7,10]. For the boiling of ethanol, the superheat degree $\Delta T = T - T_b$, where T_b is the boiling temperature, determines the mass boiling rate in Eq. (1). Using the above rates of phase change, jump conditions for mass, momentum and heat transfer at the resolved interface are given [5–7,10].

All the liquid/gas and liquid/liquid interfaces are directly captured with a fully-resolved grid system (described later). In addition to the above flow variables, level-set functions F_i are solved [5–7] using

$$\partial_t F_i + (\mathbf{u} \cdot \nabla) F_i = -|\nabla F_i| s_L, \quad (3)$$

where $s_L = \dot{\omega}/\rho_L$ is the surface regression speed due to phase change. The level-set method is combined with the MARS (Multi-interface Advection and Reconstruction Solver) method [5–7,11], a kind of VOF (Volume-Of-Fluid) method, to improve the volume conservation. Curvature is calculated using the level-set function and surface tension force is formulated by the CSF (Continuum Surface Force) method [12].

Decane ($C_{10}H_{22}$) is used as a surrogate fuel. This simplification, however, does not change the essential flow and combustion physics explored in the present study. Combustion of ethanol and decane is modeled by the global one-step chemistry mechanisms proposed in [13]. Six species, i.e. decane ($C_{10}H_{22}$), ethanol (C_2H_5OH), O_2 , N_2 , CO_2 and H_2O , are considered. As will be discussed later, SDRs are used for the analysis of flame/puffing interaction since puffing of ethanol vapor dominantly changes the local SDRs due to the ejected jet flow effect. Therefore, the change of droplet combustion characteristics by puffing is essentially not due to a chemical effect by intermediate radicals, and can be primarily captured using the above one-step chemistry mechanisms.

A decane/ethanol emulsion droplet (Case A) and a droplet group (Case B) in a hot convective air flow are considered. During the heating process, coalescence of ethanol sub-droplets generally occurs due to thermocapillary migration and reduced functionality of the surfactant. However, the characteristic time scale of this coalescence process for spray-scale droplets in a combustor is much longer than that of the puffing, and therefore droplet coalescence is not directly solved here [5–7]. Instead, the current study utilizes the research outcome of the previous study on convective heating of an emulsion droplet [6] to save computational time of the droplet heating process. The ECME (Effective Conductivity with Modified Eccentricity) method [6] is used to account for inner-droplet heating with internal circulation for the liquid Péclet number regime ($100 < Pe_L < 500$) considered in the present study. Vapor bubble nucleation is initiated by placing a tiny vapor bubble in a high-temperature region near the interface of an ethanol sub-droplet [5–7,14].

The number and size of the ethanol sub-droplets are set to be 19 and $D_{sub} = 4.6 \mu\text{m}$ as initial conditions. The diameter of the parent decane droplet is $D = 30 \mu\text{m}$. Therefore the volume fraction of ethanol is 7.4%, which typically triggers puffing rather than full microexplosion [5–7]. The ambi-

ent pressure is $p = 10 \text{ atm}$ and the temperature $T = 900 \text{ K}$. The air flow velocity is $U = 10 \text{ m/s}$, and the droplet Reynolds number is 30. In Case B, the initial relative locations of emulsion droplets, normalized by D , are $(x, y, z) = (0, 0, 0)$, $(+1.47, +0.13, +1.28)$, $(+1.47, +2.05, +0.96)$, $(-0.13, +1.09, +1.41)$, $(-1.09, +0.13, +0.96)$, $(+1.15, +2.37, -0.51)$, $(-1.09, +2.05, -0.96)$ and $(-0.45, +0.45, -1.15)$, respectively [7]. The first two droplets in the droplet group are the focus of the investigation in Section 3.2, whose inter-droplet distance is $l = 1.95D$.

The MEX (MicroEXPlosion) code is used, which has been validated in our previous studies on turbulent atomization, turbulent mixing of an evaporating spray, explosive boiling and puffing of emulsion droplets under convective heating [5–7,15,16]. The numerical scheme for advection is based on the CIP (Cubic Interpolated Pseudo-particle or Constrained Interpolation Profile) method [17]. The speed of sound is incorporated by the CUP (Combined and Unified Procedure) method [18] to include compressibility. The computational cost is higher compared with mono-component droplet combustion since the surface dynamics of not only the parent decane droplet but also the embedded ethanol sub-droplets must be resolved. The minimum grid spacing is set to be $\Delta = 0.19 \mu\text{m}$ [7] and the grid spacing is gradually stretched toward the outer rim of the computational domain. Grid convergence studies have been conducted, which confirm that the present grid spacing is fine enough to capture interface dynamics directly, including internal vapor bubble growth and surface rupture [5–7]. Structures inside the flame are also sufficiently resolved by this grid spacing. The total number of grid points is 243 million for Case A and 576 million for Case B, respectively.

3. Results and discussion

Two flame modes have been identified for mono-component droplet combustion, namely, an envelope flame and a side/wake flame [19–23]. For a certain range of droplet Reynolds numbers, multiple modes can co-exist, depending on the balance between the surface evaporation rate and convective/diffusive transport. Under the $Re = 30$ conditions, a side/wake flame will be formed at a moderate evaporation rate [19], as considered in the present study. Without puffing/microexplosion, the flame is quasi-steady in the wake of the droplet. When puffing of ethanol vapor occurs, another fuel (ethanol) is ejected repeatedly into the flame region in a short time scale and changes the flame dynamics and heat release rate. The interaction between the droplet wake flame and ejected ethanol vapor due to puffing will be discussed in detail in the following subsections.

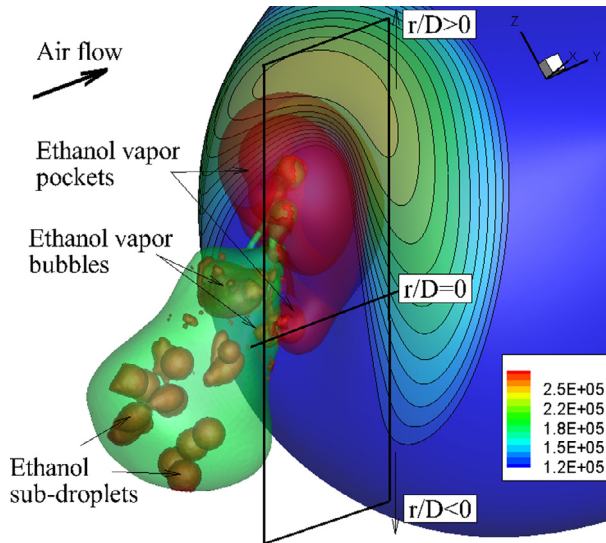


Fig. 1. Puffing and puffing-induced interaction between ejected ethanol vapor and the decane-droplet wake flame at $t = 9.2 \mu\text{s}$. The red iso-surfaces indicate $Y_{\text{ethanol}} = 0.05$ and 0.1 . The green iso-surface indicates the parent droplet surface and the dark green iso-surfaces the liquid sub-droplet shapes. The wake flame shape is illustrated by the blue iso-surface of $T = 1800 \text{ K}$ with the ethanol consumption rate ($\text{mol}/\text{m}^3/\text{s}$) superimposed (scaled by the color bar). The 2D plane is later used for data collection and analysis. (For interpretation of the references to color in this figure legend, the reader is referred to the web version of this article.)

3.1. Puffing-induced flame interaction with ejected ethanol vapor

Figure 1 shows a snapshot of puffing and puffing-induced secondary breakup for case A at $t = 9.2 \mu\text{s}$. Ethanol vapor pockets are indicated by two red iso-surfaces of $Y_{\text{ethanol}} = 0.05$ and 0.1 . A temperature iso-surface of $T = 1800 \text{ K}$ is drawn to indicate the wake flame downstream of the parent decane droplet. The time is counted from the bubble nucleation. For a droplet of $D = 30 \mu\text{m}$, the puffing time scale is $O(1 \mu\text{s})$. Ethanol vapor ejection starts at $t = 5.5 \mu\text{s}$ after bubble growth. The ejected ethanol vapor reaches the flame surface and the flame/vapor interaction starts slightly before $t = 7.8 \mu\text{s}$. At $t = 9.2 \mu\text{s}$, as shown in Fig. 1, the flame shape is locally stretched and distorted due to the progressed flame/vapor interaction.

The global characteristics of the interaction between the puffing and droplet flame is presented in Fig. 2, which shows the temporal traces of the flame surface area and heat release rate for Case A. It is clear that the puffing transiently increases the flame surface area and also the total heat release rate. As diffusion progresses, this transient effect becomes weaker. The flame surface area reaches a maximum value at $t \sim 9.4 \mu\text{s}$ in Fig. 2 and decreases thereafter until a next ethanol vapor pocket arrives. The heat release rate is reaching a maximum value at a later time instant after $t = 9.5 \mu\text{s}$ due to puffing-enhanced-mixing effects on combustion.

In addition to the above overall statistics, detailed analyses are conducted hereafter. Note that,

in the following discussion, $t = 7.8 \mu\text{s}$ indicates the time slightly after the fuel-vapor/flame interaction starts, and $t = 9.2 \mu\text{s}$ when the interaction has progressed as shown in Fig. 1. Figure 3 shows scatter plots of the gas-phase temperature, heat release rate, SDRs and mass fractions of decane and ethanol vapor during the flame/puffing interaction. These results present more quantified information about local interactions between ejected ethanol vapor and the droplet wake flame. The local flame/ethanol-vapor interaction due to puffing occurs in the flame base region. The rectangle in Fig. 1 schematically shows the data acquisition plane for the analysis. The data acquisition range in the flow direction is from $0.5D$ to $1.07D$ downstream of the parent droplet rear surface. In $r/D > 0$, where r/D is the normalized transverse distance from the droplet center, the flame/vapor interaction takes place. It can be seen that in $r/D < 0$, the effect of ethanol is minor and the wake flame is undisturbed. In contrast, in $0.2 < r/D < 0.9$ at $t = 7.8 \mu\text{s}$ and $0.2 < r/D < 1.2$ at $t = 9.2 \mu\text{s}$, the interaction with the ethanol vapor has changed the flame base structure. The upstream gas-phase temperature in the interaction region becomes lower due to the impact of ejected ethanol vapor ($Y_{\text{ethanol}} = 1$ and $T \sim 425 \text{ K}$). The ethanol mass fraction is close to the stoichiometric value around $r/D \sim 0.9$ at $t = 7.8 \mu\text{s}$ and $r/D \sim 1.2$ at $t = 9.2 \mu\text{s}$, which makes the peak value of the heat release rate of ethanol comparable to that of decane. Basically, vapor ejection is governed by the convective jet effect when puffing

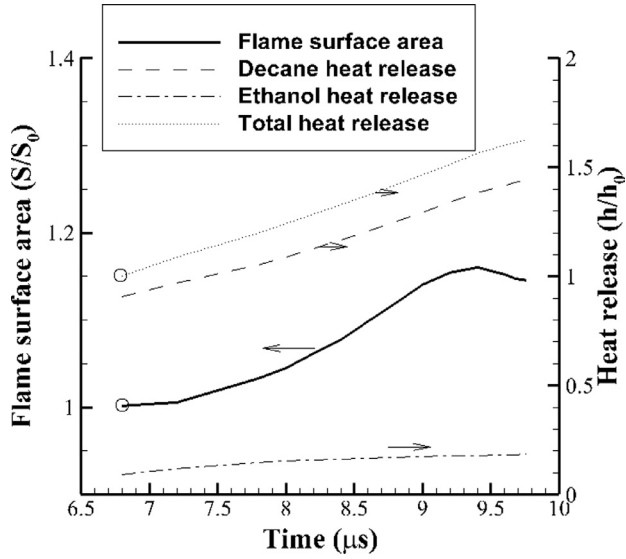
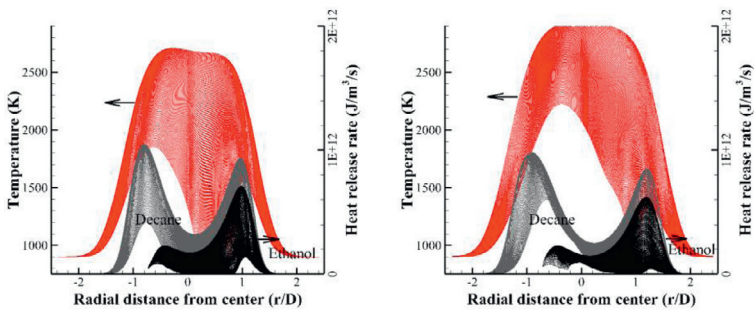
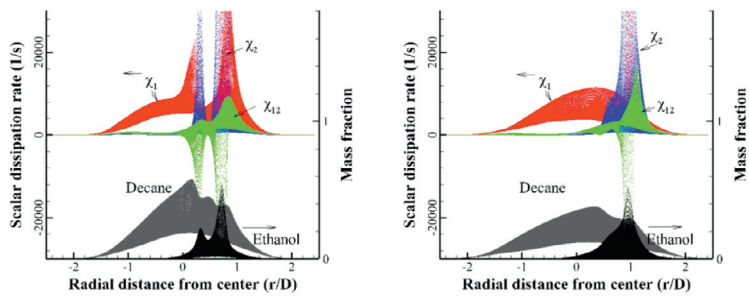


Fig. 2. Temporal traces of flame surface area S and heat release rate h , which are normalized by S_0 and h_0 (indicated by the circles) at $t = 6.8 \mu\text{s}$, respectively.



(a) gas-phase temperature and heat release rates at $t=7.8\mu\text{s}$ (left) and $t=9.2\mu\text{s}$ (right)



(b) scalar dissipation rates and fuel vapor mass fractions at $t=7.8\mu\text{s}$ (left) and $t=9.2\mu\text{s}$ (right)

Fig. 3. Scatter plots of gas-phase temperature, heat release rate, scalar dissipation rates and mass fractions of decane and ethanol vapor in the flame base region.

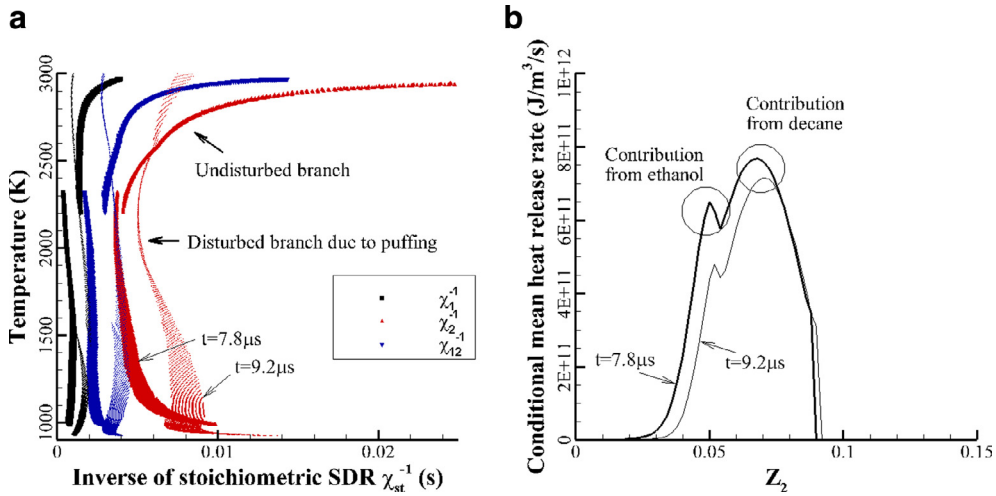


Fig. 4. Flame structure on the stoichiometric surface under puffing. (a) S-curves where the large symbols indicate values at $t = 7.8 \mu s$, and the small ones at $t = 9.2 \mu s$. (b) Conditional mean heat release rate $(\dot{\omega}|Z_2)_{st}$ on the stoichiometric surface of the disturbed flame.

starts and diffusion gradually takes place after the ejection. At $t = 9.2 \mu s$, the diffusion effect is relatively stronger than at $t = 7.8 \mu s$.

For an evaporating fuel droplet with combustion, a mixture fraction is defined to incorporate the effect of diffusion and chemical reaction as $Z_i = (Y_{F,i} + (Y_{O_2,0} - Y_{O_2})/s_i)/(1 + Y_{O_2,0}/s_i)$ for a one-step global reaction of $F_i + s_i O \rightarrow (1 + s_i) P_i$ [24], where the subscript 0 denotes a value at the far field and $Y_{F,0} = 1$ is used. F_i , O and P_i stand for fuel, oxidizer and product, respectively. s_i is the mass ratio of oxidizer to fuel at the stoichiometric condition. The subscript $i = 1$ denotes decane and $i = 2$ ethanol. For a dual-fuel system, three SDRs are defined, namely, $\chi_1 = 2D_{dif}|\nabla Z_1|^2$, $\chi_2 = 2D_{dif}|\nabla Z_2|^2$, $\chi_{12} = 2D_{dif}(\nabla Z_1 \cdot \nabla Z_2)$, where D_{dif} is the diffusion coefficient [7,25]. A unity Lewis number is assumed here. χ_1 represents mixing/reaction between decane and air, χ_2 between ethanol and air, and χ_{12} cross mixing between decane and ethanol. Figure 3b shows the distribution of χ_1 , χ_2 and χ_{12} on the plane shown in Fig. 1. In $0.0 < r/D < 1.0$ ($t = 7.8 \mu s$) and $0.0 < r/D < 1.2$ ($t = 9.2 \mu s$), where the flame interacts with the ejected ethanol vapor, it is evident that the ethanol vapor locally increases the magnitude of the SDRs. χ_1 and χ_2 are always positive and indicate the normal mixing between the respective fuel and air. χ_{12} quantifies the cross mixing between the two fuels, which is particular to puffing [7]. χ_{12} can be both positive and negative depending on the local flow structures. Puffing initially makes χ_{12} mostly negative, since the ethanol vapor is ejected into the decane-vapor/air mixture by the jet motion and generates opposed stratification of the two fuels, which is also observed in non-reacting cases [7]. As the coupling between diffusion and

local convection becomes gradually stronger, χ_{12} can be also positive.

Figure 3 indicates that puffing of ethanol vapor changes the local SDRs dominantly due to the ejected jet effect, where the local strain and the spatial gradients of fuels are increased. This necessitates quantification of the effects of multiple SDRs on the flame dynamics in further detail, which is discussed next.

The correlations between the gas-phase temperature and SDRs on the stoichiometric surface (S-curves [26]) are presented in Fig. 4a, which further show the puffing effect on droplet combustion. The region investigated is $r/D > 0$ shown in Fig. 1. The flow-direction length of the rectangle is extended further downstream to $2.0D$ to include an undisturbed (not significantly affected) flame region for comparison purposes. On the upper side of the figure, the undisturbed flame (the upper branch of the S-curves) can be seen, where the flame temperature is lower for smaller χ_{st}^{-1} . On the lower-left side of the figure, the flame region strongly affected by puffing can be seen. The puffing-affected flame branch is discontinuous from the undisturbed upper branch. The SDRs are increased by puffing (see Fig. 3b) and accordingly the gas-phase temperature is lower. The puffing is, however, not strong enough to cause extinction. Figure 4b shows the conditional mean heat release rate at the stoichiometric condition, $(\dot{\omega}|Z_2)_{st}$, of the disturbed flame in the puffing region. Two peaks can be found. The DNS data show that the main contribution from decane is formed around $Z_2 \sim 0.07$ and the contribution from ethanol makes the second peak around $Z_2 \sim 0.05$. Figure 4 indicates that the flame structure is different from that of a one-dimensional (1D) flame for a single fuel, and suggests that the mod-

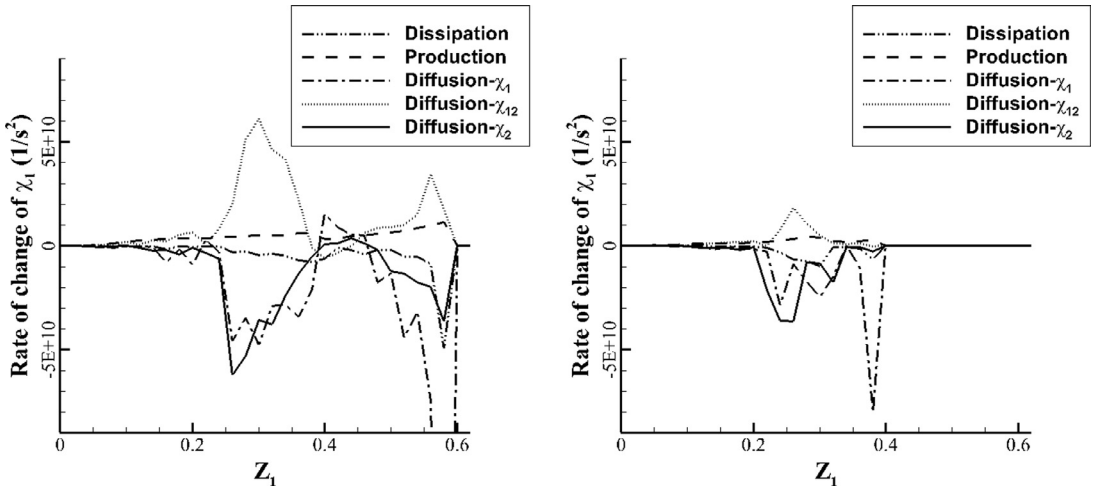


Fig. 5. Contribution of each term on the RHS of Eq. (4) to the rate of change of χ_1 at $t = 7.8 \mu\text{s}$ (left) and $t = 9.2 \mu\text{s}$ (right).

eling of the puffing effect is possible in the $Z-\chi$ space.

The SDR is a key quantity in non-premixed flame modeling. To better understand the puffing effects due to the secondary fuel ethanol on the SDR of the primary fuel decane, the SDR transport equation for decane is analyzed, which is [25]

$$\frac{\partial \chi_1}{\partial t} = -\frac{1}{4} \left(\frac{\partial \chi_1}{\partial Z_1} \right)^2 + 2a\chi_1 + \left(\frac{\chi_1}{2} \frac{\partial^2 \chi_1}{\partial Z_1^2} + \chi_{12} \frac{\partial^2 \chi_1}{\partial Z_1 \partial Z_2} + \frac{\chi_2}{2} \frac{\partial^2 \chi_1}{\partial Z_2^2} \right) + S_{\chi_1}. \quad (4)$$

It should be noted that this equation is a model budget equation to quantify the effects of each term in the $Z-\chi$ space. The terms on the right-hand side (RHS) represent dissipation, production, diffusion of decane, cross diffusion between decane and ethanol, diffusion of ethanol, and evaporation source, respectively. a is the dominant compressive strain rate. Figure 5 shows the contribution of each RHS term to the rate of change of χ_1 conditionally averaged on Z_1 , i.e. $\partial \langle \chi_1 | Z_1 \rangle / \partial t$. The source term is dominant only in the very vicinity of the surface of the parent decane droplet, and therefore excluded from the gas-phase analysis here. Once mixing starts, following the initial stratification generated by ethanol vapor ejection, the diffusion terms due to χ_1 and χ_2 contribute negatively to $\partial \langle \chi_1 | Z_1 \rangle / \partial t$, which indicates normal diffusion processes. The cross mixing term due to χ_{12} mostly contributes positively to $\partial \langle \chi_1 | Z_1 \rangle / \partial t$, which is particular to the ejected ethanol vapor. The net contribution of the RHS terms to $\partial \langle \chi_1 | Z_1 \rangle / \partial t$ is negative and therefore χ_1 decreases gradually, which means the steep gradients produced by puffing are attenuated by mixing and reaction. This trend is qualitatively similar to that observed in non-reacting cases

[7]. The above results indicate that the dual-fuel vapor field including puffing can be considered in the framework of the conservative mixture fractions Z_i for both reacting and non-reacting cases.

3.2. Droplet group combustion under puffing

Puffing in the transverse direction has a transient effect on droplet grouping when there are other droplets in the neighborhood. The modulation of droplet grouping by puffing has been confirmed in non-reacting cases [7]. The previous study [7] on the ethanol-vapor pocket trajectory by tracking the center of gravity of a vapor pocket in non-reacting cases has unveiled that the trajectory is similar to that of a jet in crossflow, i.e. $x_{ir} \sim x_d^\alpha$, where $\alpha = 1/3 \sim 1/2$, x_{ir} is the transverse distance and x_d is the downstream distance [7,27]. This correlation applies for a certain range of the equivalent ejection speed ratio $r = \sqrt{\rho_v u_v^2 / \rho_m u_m^2}$, where the subscripts v and m represent the vapor jet velocity and the main air flow velocity, respectively. In Case A where the droplet wake flame is affected by puffing, r is around 3.3, and the vapor pocket trajectory is similar to that for the corresponding non-reacting case [7] (not shown here). This is expected since the initial stage of vapor ejection is dominantly determined by jetting for both reacting and non-reacting cases. It indicates that the ejected ethanol vapor pockets may reach a few diameters away from the parent decane droplet, induce interdroplet interaction and modulate droplet group combustion when there are other droplets in this region of influence.

For Case B, the puffing dynamics and flame modulation due to puffing are similar to those for Case A. Figure 6 shows a snapshot of interactions between puffing and the droplet-group flames in

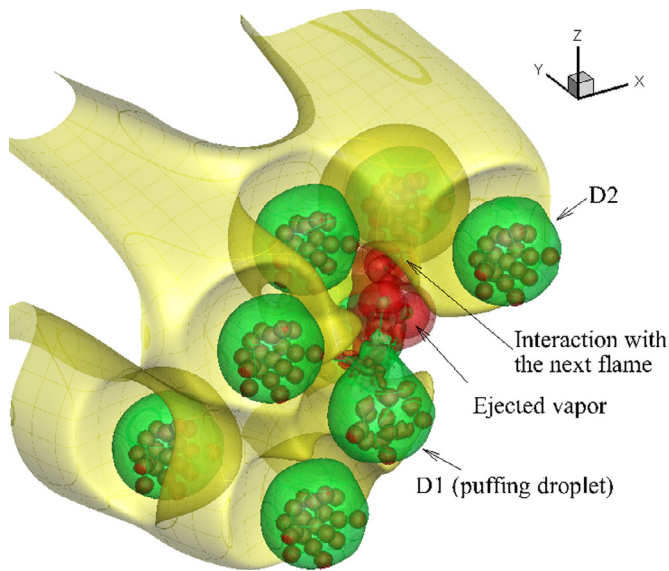


Fig. 6. Droplet group combustion under puffing (Case B). See Fig. 1 for iso-surface definitions. The yellow iso-surface represents $T = 1800$ K. In the x and z directions, periodic boundary conditions are imposed. (For interpretation of the references to color in this figure legend, the reader is referred to the web version of this article.)

Case B, where inter-droplet interactions occur and affect the droplet-grouping mode due to puffing. Each flame is similarly formed in the wake of a droplet. Between the two droplets on the upstream side (D1 and D2 as shown in Fig. 6), puffing of an ethanol vapor pocket can be seen. Since the inter-droplet distance is small ($l = 1.95D$) and within the region of influence, the ethanol vapor pocket impacts on both flames of D1 and D2. Puffing can therefore be an additional transient factor affecting droplet grouping, in addition to static droplet settings such as geometrical droplet positions and flow conditions [19–23,28]. The group combustion theory has been developed based on steady conditions [29], but it has been first demonstrated here in detail that transient effects such as puffing can also be important for emulsion fuels. For such fuel blends, DNS can be a powerful tool, as shown in the present study, to guide the modeling of emulsion-fuel spray combustion.

4. Concluding remarks

Combustion characteristics of an emulsion droplet and a droplet group have been investigated to elucidate puffing-induced interaction between ejected ethanol vapor and a wake droplet flame. Puffing occurs in a short time scale and the ejected ethanol vapor rapidly reaches the flame base. The ethanol vapor interacts with the flame by transiently increasing the flame surface area and heat release rate for a certain period. The impacted region by puffing exhibits different temperature and reac-

tion rate characteristics from a 1D flame. The SDRs are strongly affected by the ejected ethanol vapor due to its jet flow effect. The flame S-curves indicate that the combustion characteristics are also affected by the change in the SDRs. The puffing effect can be quantified by the budget analysis in the $Z-\chi$ space. The SDR due to cross mixing between the primary fuel decane and the secondary fuel ethanol is dominantly negative, which is particular to puffing. As mixing progresses, the cross SDR can be also positive, since the overall spatial gradients of decane and ethanol vapor may align with the same direction. Then the magnitude of the SDRs reduces, as indicated by the budget analysis. When the vapor ejection is toward the transverse direction, it has an influence in a region whose span is within a few diameters from the puffing parent droplet. In the multiple-droplet configuration, the inter-droplet interaction can be enhanced and droplet group combustion can be modulated by puffing transiently. Therefore, puffing is an additional factor in the droplet grouping even when the geometrical configuration of the droplet group remains unchanged. Such an insight gained from the present DNS study is crucially important for accurately modeling combustion of biofuel-blended emulsion-fuel sprays.

Acknowledgments

Financial support from the Engineering and Physical Sciences Research Council (EPSRC) of the UK under the Grant no. EP/J018023/1 is

gratefully acknowledged. This work used the ARCHER UK National Supercomputing Service (<http://www.archer.ac.uk>). Computing resources on ARCHER were provided by the UK Consortium on Turbulent Reacting Flows (UKCTRF).

References

- [1] A.K. Agarwal, *Prog. Energy Combust. Sci.* 33 (2007) 233–271.
- [2] S.A. Shahir, H.H. Masjuki, M.A. Kalam, A. Imran, I.M. Rizwanul Fattah, A. Sanjid, *Renew. Sust. Energy Rev.* 32 (2014) 379–395.
- [3] M.L. Botero, Y. Huang, D.L. Zhu, A. Molina, C.K. Law, *Fuel* 94 (2012) 342–347.
- [4] T. Kadota, H. Yamasaki, *Prog. Energy Combust. Sci.* 28 (2002) 385–404.
- [5] J. Shinjo, J. Xia, L.C. Ganippa, A. Megaritis, *Phys. Fluids* 26 (2014) 103302.
- [6] J. Shinjo, J. Xia, A. Megaritis, L.C. Ganippa, R.F. Cracknell, *Atom. Sprays* 26 (2016) 551–583.
- [7] J. Shinjo, J. Xia, L.C. Ganippa, A. Megaritis, *J. Fluid Mech.* 793 (2016) 444–476.
- [8] H. Watanabe, K. Okazaki, *Proc. Combust. Inst.* 34 (2013) 1651–1658.
- [9] NIST web database available at <http://webbook.nist.gov/chemistry/fluid/>
- [10] S. Tanguy, T. Menard, A. Berlemont, *J. Comput. Phys.* 221 (2007) 837–853.
- [11] T. Kunugi, *J. Jpn. Soc. Mech. Eng. B* 63 (1997) 1576–1584.
- [12] J.U. Brackbill, D.B. Kothe, C. Zemach, *J. Comput. Phys.* 100 (1992) 335–354.
- [13] C.K. Westbrook, F.L. Dryer, *Combust. Sci. Technol.* 27 (1981) 31–43.
- [14] C.T. Avedisian, R.P. Andres, *J. Colloid Int. Sci.* 64 (1978) 438–453.
- [15] J. Shinjo, A. Umemura, *Int. J. Multiph. Flow* 36 (2010) 513–532.
- [16] J. Shinjo, J. Xia, A. Umemura, *Proc. Combust. Inst.* 35 (2015) 1595–1602.
- [17] H. Takewaki, A. Nishiguchi, T. Yabe, *J. Comput. Phys.* 61 (1985) 261–268.
- [18] T. Yabe, F. Xiao, T. Utsumi, *J. Comput. Phys.* 169 (2001) 556–593.
- [19] H.H. Chiu, J.S. Huang, *Atom. Sprays* 6 (1996) 1–26.
- [20] H.A. Dwyer, B.R. Sanders, *Proc. Combust. Inst.* 21 (1986) 633–639.
- [21] G. Wu, W.A. Sirignano, F.A. Williams, *Combust. Flame* 158 (2011) 1171–1180.
- [22] G. Wu, W.A. Sirignano, *Combust. Flame* 158 (2011) 2395–2407.
- [23] W.A. Sirignano, *Prog. Energy Combust. Sci.* 42 (2014) 54–86.
- [24] R.W. Bilger, *Combust. Flame* 158 (2011) 191–202.
- [25] C. Hasse, N. Peters, *Proc. Combust. Inst.* 30 (2005) 2755–2762.
- [26] N. Peters, *Turbulent Combustion*, Cambridge University Press, Cambridge, U.K., 2000, pp. 3–5.
- [27] S. Muppidi, K. Mahesh, *J. Fluid Mech.* 530 (2005) 81–100.
- [28] M.R.G. Zoby, S. Navarro-Martinez, A. Kronenburg, A.J. Marquis, *Proc. Combust. Inst.* 33 (2011) 2117–2125.
- [29] H.H. Chiu, H.Y. Kim, E.J. Croke, *Proc. Combust. Inst.* 19 (1982) 971–980.